Evaluation of small-strain shear stiffness of soil under anisotropic stress state for vertically propagating shear waves

Piotr Kowalczyk, Ph.D.,[1] and Oliver Fiddaman[2]

[1] Currently Independent Researcher (Marie Skłodowska-Curie Postdoctoral Fellow from 2027), orcid: 0000-0003-0777-6429; email: piotr.kowalczyk.research@protonmail.com (Corresponding author)

[2]Senior Laboratory Technician, Structural Soils Ltd, Stillhouse Ln, Bristol BS3 4EB, United Kingdom; email: oliver.fiddaman@soils.co.uk

ABSTRACT:

Research studies using centrifuge modelling is a prime choice for investigation of soil-structure interaction in earthquake geotechnical engineering. Centrifuge studies are most effective when supported by complementary numerical modelling aimed at conducting expanded parametric studies. The numerical studies use soil constitutive models which need to be calibrated against soil element tests representing the dominant stress paths, stress and strain levels induced in centrifuge models. Currently, there is a gap in the available laboratory data with no database on the small-strain shear stiffness of soil subjected to anisotropic consolidation, thus accurate calibration of soil constitutive models for vertically propagating shear waves in centrifuge is not possible. This work presents results from soil laboratory tests to address this gap and provide a new dataset on the small-strain shear stiffness of soil subjected to anisotropic consolidation compared with tests under an isotropic stress state. To this aim, resonant column tests, supported by small-strain torsional shear tests, were conducted on triaxial samples under a range of different stress and strain levels representative of those observed in centrifuge tests on shear wave propagation. The results show that the initial small-strain stiffness is primarily governed by the vertical stress component. The difference in the shear stiffness degradation G/G_0 between corresponding anisotropically and isotropically consolidated samples increases with increasing shear strain. Recommendations for using simple analytical expressions for evaluating the small-strain stiffness characteristics of soil under anisotropic consolidation are provided.

PRACTICAL APPLICATIONS:

Finite element modelling in geotechnical engineering relies on calibration of soil constitutive models on soil laboratory tests. Many geotechnical problems including urban construction (tunnels, deep excavations, retaining walls), offshore and seismic geotechnics, strongly depend on accurate modelling of soil mechanical behavior at small strains. In case of numerical models simulating structural performance to earthquake loading, it is soil deformation to the vertically propagating shear waves which is critical and needs to be captured accurately. This work provides a new dataset of soil laboratory tests on soil mechanical behavior under stress and strain levels induced by seismic shear waves, in particular, including cases of anisotropic soil consolidation, which is always a case in centrifuge models and often on real sites subjected to earthquake loading. The results from anisotropically consolidated samples are compared with isotropically consolidated samples and show that: i) the vertical stress component is dominant for the initial shear stiffness G_0; ii) the difference in the shear stiffness degradation G/G_0 between anisotropic and isotropic stress states increases with increasing shear strain. Recommendations are provided for the use of simple analytical expressions. The relevance of the new dataset beyond the numerical modelling of centrifuge testing in earthquake engineering is briefly discussed.

AUTHOR KEYWORDS: small-strain stiffness, anisotropic consolidation, resonant column testing, shear wave propagation, soil dynamics, centrifuge modelling, finite element modelling, soil element testing, sand.

INTRODUCTION:

Small-scale physical modelling in a geotechnical centrifuge has been proved to be an effective method to identify physical mechanisms when investigating soil-structure interaction, including cases when seismic loading is applied (see examples in Table 1). Centrifuge experimental studies are often accompanied by complementary numerical studies to expand the investigation with comprehensive parametric studies not restricted to a limited number of centrifuge tests. Past numerical models for cases of research on dry sand (see examples in Table 2) were calibrated against centrifuge studies due to the limited availability of relevant laboratory data. In contrast, ideally one would want to have a three-component methodology, with numerical studies calibrated before centrifuge runs against soil element tests representative of the stress and strain levels expected to be experienced in a physical model. This is sometimes the case for research on saturated sand subject to liquefaction (e.g., He et al., 2020; Özcebe et al., 2021; Mercado et al., 2024), however, is outstanding for cases of dry sand.

There are a limited number of research works which present useful soil element tests on which soil constitutive models aimed at replicating centrifuge experiments under seismic loading in dry sand can be calibrated. Lanzano et al. (2016) conducted resonant column tests on Leighton Buzzard sand to assess the initial shear stiffness G_0 and its degradation within the small-strain range of up to 0.1%. Subsequent work by Kassas et al. (2021) included conducting a suite of bender element tests on triaxial samples to determine the G_0 value of Hostun sand for the purpose of calibration of soil constitutive models when replicating soil behavior in centrifuge studies. Nevertheless, these two works assumed the stress state to be isotropic and, thus, not representative of the actual stress state in centrifuge studies where normally K_0 conditions are achieved (e.g., Tsinidis et al., 2015). An exception of soil element testing on samples on dry sand subjected to anisotropic consolidation are recent research works by Lbibb & Manzari (2022) and Kowalczyk & Madhusudhan (2025). However, the former work gives only a couple of G_0 values estimated from bender element tests for samples under vertical confining stresses of 40 and 100kPa. The latter focused on low vertical effective stresses of less than 20kPa since aimed on improved understanding of soil behavior in physical modelling under 1-g conditions, thus its use for calibration of soil constitutive models at higher stress levels is not possible.

Table 1 Examples of centrifuge testing used in research in earthquake geotechnical engineering.

Reference	**N-g level**	**Depth of the soil in the model [m]**	**Relative density D_r of sand [%]**
Lanzano et al. (2012)	80/40	24/12	40, 75
Abuhajar et al. (2015)	60	20	50, 90
Madabhushi & Haigh (2022)	60	10.5/16.5	80-85
Fusco et al. (2024)	60	15	50
Zhang et al. (2024)	60	20	56, 66
Asia et al. (2025)	60	20	40
He et al. (2025)	60/80	20-24	50
Wei et al. (2026)	50	20	80

Table 2 Examples of the research works based on integrated centrifuge and numerical methodology for cases of soil-structure interaction in dry sand.

Subject of the study	Constitutive model	Selected calibration method	Reference
Circular tunnels	Hardening Mohr-Coulomb in Abaqus	Not clarified	Cilingir & Madabhushi (2010)
Square tunnels	Mohr-Coulomb in Abaqus	Not clarified	Cilingir & Madabhushi (2011)
Buried box culverts	Mohr-Coulomb in Flac	On centrifuge studies	Abuhajar et al. (2015)
Dual-row retaining wall	Mohr-Coulomb in Swandyne software	On centrifuge studies	Madabhushi & Haigh (2022)
Dynamic earth pressures on rigid walls	SANISAND model (Dafalias & Manzari, 2004)	Monotonic drained triaxial tests, recalibrated subsequently against centrifuge data	Madabhushi & Westcott (2024)

Although ideally soil constitutive models calibrated against a particular set of soil element tests should be able to replicate soil response in other soil element tests, this is often not the case (e.g., Wichtmann et al., 2019). Bearing in mind that shear wave velocity depends on whether the stress state is isotropic or anisotropic (e.g., Fioravante, 2000), calibration of soil constitutive models against soil element tests conducted at an isotropic stress state is uncertain when applied to numerical models of centrifuge tests run at anisotropic consolidation. As a result, it appears there is a gap in the currently available laboratory data and soil element tests evaluating the small-strain stiffness for vertically propagating shear waves in anisotropically stressed soil are not available when calibrating soil constitutive models for comprehensive research studies combining centrifuge and numerical research approaches.

Previous laboratory studies are of limited applicability for the calibration of soil constitutive models in numerical simulations of shear wave propagation. Most typically, soil element testing focused on the small-strain stiffness characteristics is carried out on isotropically consolidated samples (e.g., Lanzano et al., 2016; Wichtmann & Triantafyllidis, 2016; Rohilla & Sebastian, 2023). Sometimes, anisotropic stress states are considered. For example, Santamarina & Cascante (1996) studied shear wave propagation in soil samples under stress-induced anisotropy, however the anisotropic stress state was achieved by application of axial compression or extension to samples which were firstly isotropically consolidated. Similar testing procedure was followed by Goudarzy et al. (2018a), where a number of stress paths were investigated, including anisotropic stress states obtained from initially isotropic consolidation, thus not representative of normally consolidated soil where K_0 is constant during consolidation, as is the case in centrifuge or in field. Table 3 summarizes previous studies on dry sand involving anisotropic stress states and highlights their limitations.

This work presents a suite of torsional resonant column tests and small-strain static torsional shear tests of dry sand subjected to truly anisotropic consolidation. The results from anisotropically consolidated samples are compared with tests carried out at isotropic consolidation pressures. The conducted tests are focused on the stress path of simple shear deformation and are carried out in the range of small strains, thus they are highly applicable in understanding shear wave propagation in boundary value problems in earthquake geotechnical engineering and, consequently, critical for accurate calibration of macroscopic continuum-based soil constitutive models dedicated to modelling of centrifuge tests or cases of predictive design in earthquake geotechnical engineering.

Table 3 Summary of experimental research on dry sand under anisotropic stress state and small-strain stiffness.

Reference	Laboratory test type	How anisotropy considered	Limitations with respect to seismic/centrifuge studies
Santamarina & Cascante (1996)	Resonant column	Isotropically consolidated sample subjected to axial extension or compression	No truly anisotropic consolidation; tests on Barco sand 32 (not used in centrifuge)
Fioravante (2000)	Bender element testing	Truly anisotropic consolidation for K ranging from 0.33 to 2.0	Data on stiffness degradation G/G_0 not provided; tests on Ticino sand and Kenya sand
Goudarzy et al. (2018a)	Resonant column	Isotropically consolidated sample subjected to anisotropic stress state	No truly anisotropic consolidation
Lbibb & Manzari (2022)	Bender element testing	Truly anisotropic consolidation achieved in a direct simple shear device	Data on stiffness degradation G/G_0 not provided; only a couple of G_0 values determined
Kowalczyk & Madhusudhan (2025)	Direct simple shear testing	Truly anisotropic consolidation	Tests limited to low effective stresses below 20kPa

METHODOLOGY

A state-of-the-art resonant column apparatus (Werden et al., 2013) was used to carry out torsional resonant column tests (example of a tested sample in the used apparatus is shown in Figure 1a). This device is also capable of carrying out static torsional shear tests, which were also used in the presented work. The testing system is a fully automated system able to measure the shear modulus and damping of soils at strains down to 10^{-6}. In contrast to other systems, the measurements of the direct torque are made at the bottom of the soil specimen.

The laboratory tests were conducted on dense and medium dense dry sand. In fact, these two relative densities are most often used in centrifuge studies (see examples in Table 1). Dry pluviation with tamping was used to achieve the required density in a sample of the nominal dimensions of 70mm (diameter) by 140mm (height). Summary of the conducted tests is shown in Table 4. Hostun sand was selected as often used also in centrifuge studies (e.g., Tsinidis et al., 2015; Madabhushi & Haigh, 2019; Deng & Haigh, 2021; Kassas et al., 2021; Morley et al., 2024; Fusco et al., 2024; Asia et al., 2025). Hostun sand is an angular to sub-angular fine sand with a mean particle diameter D_{50} of 0.341mm and the coefficient of uniformity C_u of 1.47 (Adamidis et al., 2020; Kassas et al., 2021). The particle size distribution of Hostun sand is shown in Figure 1b.

The prepared samples were tested in a multistage mode shown to be successful in previous research studies using resonant column testing (e.g., Payan et al., 2016; Goudarzy et al., 2018a; Goudarzy et al., 2018b) with the vertical stress σ_v varying in the range of 20kPa to 300kPa to represent the stress levels induced in centrifuge tests (Figure 1c), and applicable also to predictive numerical studies for the purpose of design to earthquake loading. Bearing in mind the importance of the induced stress paths on soil mechanical response, two different stress paths were considered in the conducted multistage tests to replicate the soil response in truly anisotropic and isotropic consolidation (Fig. 1d). The maximum selected vertical stress of 300kPa would represent the stress state of sand of dry density ρ of 1500kg/m^3 at a depth of 20m which is often the limiting depth in centrifuge studies (e.g., Abuhajar et al., 2015; Tsinidis et al., 2015; Morley et al., 2024) and in engineering practice. The maximum strain levels to which the samples were tested under resonant column and torsional simple shear tests were selected following preliminary tests, with the aim to be: i) representative of deformation to the propagation of shear waves in centrifuge works; and to ii) avoid sample deterioration. As a result of the latter, the strain level induced at lower mean effective stresses has been reduced to avoid sample deterioration. Note that such reduction in shear strains generally takes place also in reality as a result of the zero-strain boundary condition at the top of the soil surface due to the vanishing soil strength with reducing mean effective stress (e.g., Kowalczyk & Gajo, 2023). An example of two resonant column tests on the same soil sample is shown in Figure 2 to present that the sample did not change its stiffness characteristics due to the previously applied shear strains. All resonant column tests are summarized in Table 4.

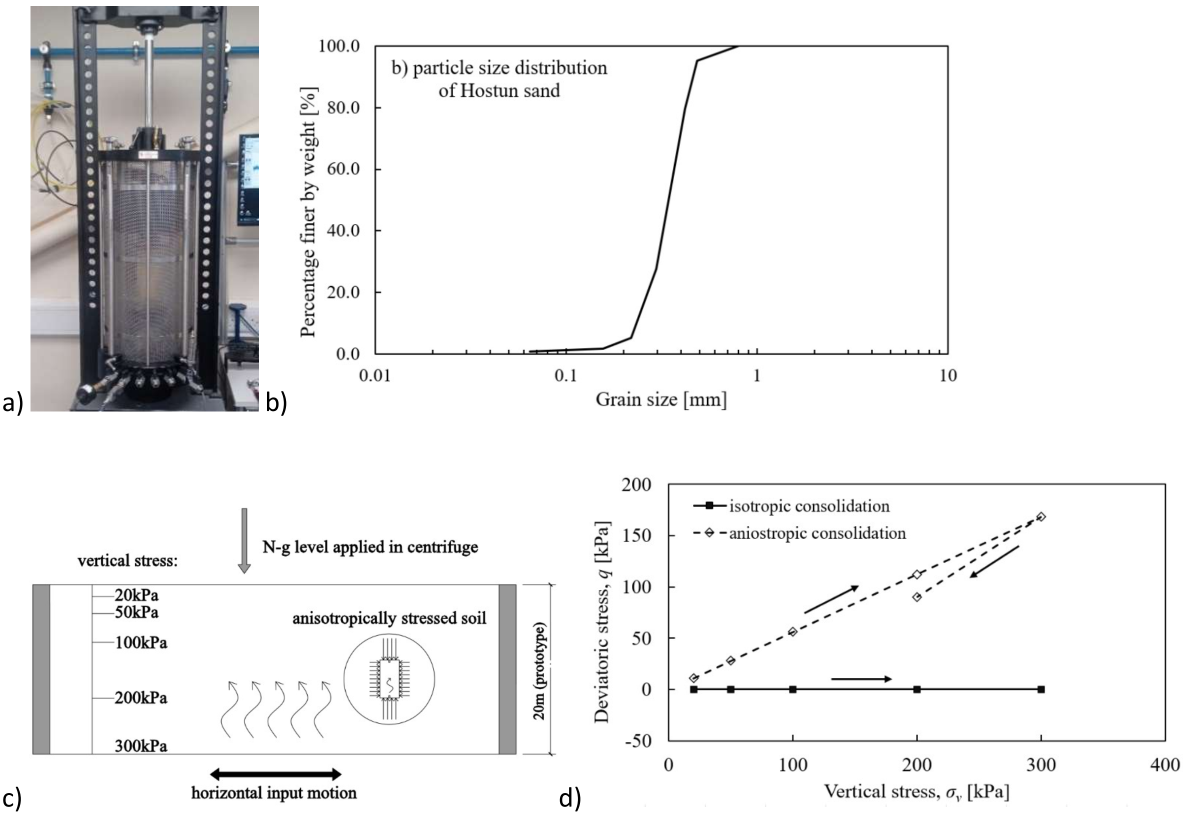

Fig. 1 a) sample installed in a resonant column apparatus, b) particle size distribution of Hostun sand, c) sketch of an example scaled model tested in a geotechnical centrifuge facility (vertical stress levels at corresponding depths estimated for dry density of ρ=1500kg/m^3, d) applied stress paths in multistage resonant column tests.

157 Table 4 Summary of the conducted multistage resonant column tests on dense Hostun sand.

Test no.	Relative density, D_r [-]	Vertical stress, σ_v [kPa]	Horizontal stress, σ_h [kPa]	Mean effective stress, p [kPa]	Max strain level, γ_{max} [%]	OCR
T1.1	0.85	20	9	12.5	0.01	1.0
T1.2	0.85	50	22	31.3	0.02	1.0
T1.3	0.85	100	44	62.7	0.03	1.0
T1.4	0.85	200	88	125.3	0.04	1.0
T1.5	0.85	300	132	188	0.05	1.0
T1.6	0.85	200	110	140	0.04	1.5
T2.1	0.8	20	20	20	0.01	1.0
T2.2	0.8	50	50	50	0.02	1.0
T2.3	0.8	100	100	100	0.03	1.0
T2.4	0.8	200	200	200	0.04	1.0
T2.5	0.8	300	300	300	0.05	1.0
T3.1	0.55	20	9	12.5	0.004	1.0
T3.2	0.55	50	22	31.3	0.006	1.0
T3.3	0.55	100	44	62.7	0.02	1.0
T3.4	0.55	200	88	125.3	0.03	1.0
T3.5	0.55	300	132	188	0.05	1.0

T3.6	0.55	200	110	140	0.04	1.5
T4.1	0.55	20	20	20	0.01	1.0
T4.2	0.55	50	50	50	0.02	1.0
T4.3	0.55	100	100	100	0.03	1.0
T4.4	0.55	200	200	200	0.04	1.0
T4.5	0.55	300	300	300	0.05	1.0

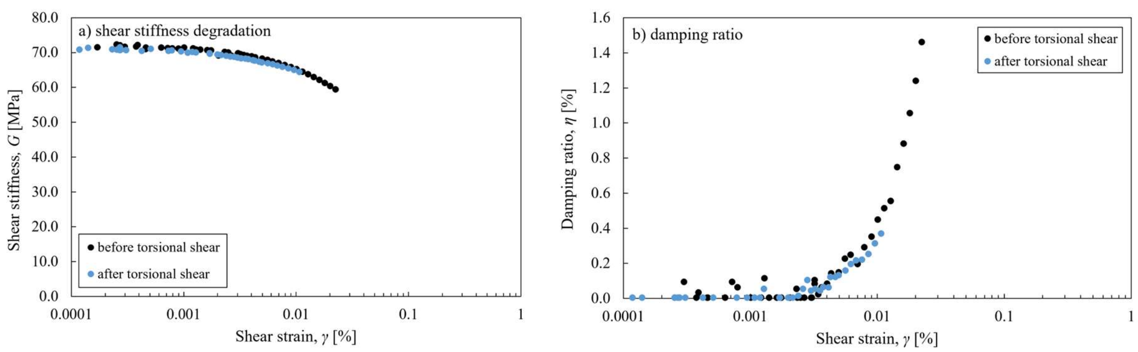

Fig. 2 Example comparison of resonant column tests carried out at the same soil sample at constant vertical effective stress of 100kPa: a) shear stiffness degradation with increasing strain, b) damping ratio.

The tests under anisotropic consolidation were carried out with the horizontal stress being a K_0 proportion of the vertical stress (see Figure 1d). K_0 was assumed as 0.44 from the Jaky's formula (1948) when using the critical friction angle φ_{cr} of 34° for Hostun sand (Deng & Haigh, 2021). The resonant column tests were carried out up to the limiting maximum shear strain level of less than 0.1%. The maximum shear strains induced in centrifuge works on shear wave propagation in dry sand have been shown to reach up to 0.1-0.3% (0.1% in Lanzano et al., 2016; 0.2% in Madabhushi & Westcott, 2024; 0.3% in Wei et al., 2026), therefore additional runs of static torsional shear tests were carried out to evaluate soil mechanical response at higher strain ranges. No filtering was applied to the measurements; only occasional outliers were removed for clarity.

Note that, although efforts have been made to conduct laboratory tests representative of vertically propagating shear waves in dry sand, the experimental campaign is limited to tests on a single sand type, two relative densities and selected strain and stress levels. Future works can address other types of soils, wider range of relative densities, strain and stress levels, beyond those investigated in this work.

In addition to anisotropic and isotropic consolidation, the influence of overconsolidation was investigated for cases when a centrifuge model is run firstly at higher n-g level and subsequently at lower n-g level as this is sometimes the case in centrifuge testing (e.g., Lanzano et al., 2012) in which case soil becomes overconsolidated. The imposed horizontal stresses for cases with overconsolidation have been computed using the formula:

$$K_{0,OCR} = (1 - sin\varphi) \cdot OCR^{sin\varphi} \qquad \text{(eq. 1)}$$

The measured soil stiffness G_0 has been compared with selected analytical expressions, including the early proposed one given by Hardin & Black (1966):

$$G_0 = A \cdot F(e) \cdot p_a \cdot \left(\frac{p}{p_a}\right)^n \qquad \text{(eq. 2)}$$

Where *A* and *n* are the fitting parameters, p_a is atmospheric pressure, and *F(e)* is a function of the void ratio *e* in the following form:

$$F(e) = \frac{(c-e)^2}{1+e} \qquad \text{(eq. 3)}$$

With *c*=2.97 for angular sands.

Moreover, expression by Yu & Richart (1984) has been used:

$$G_0 = A \cdot F(e) \cdot p_a \cdot \left(\frac{\sigma_v}{p_a}\right)^{n_1} \cdot \left(\frac{\sigma_h}{p_a}\right)^{n_2} \qquad \text{(eq. 4)}$$

With n_1 and n_2 being the fitting parameters accounting for the impact of the vertical (σ_v) and horizontal (σ_h) stress components in anisotropically consolidated samples. Note that to simplify the notation the apostrophe for describing the effective stresses is omitted in this work.

To facilitate calibration of soil constitutive models aimed at capturing shear wave propagation, e.g., a simple model by Darendeli (2001) used in site response analysis (e.g., Hashash et al., 2010) or an advanced soil constitutive model by Benz (2006) and Benz et al. (2009) accounting for hysteresis within the nonlinear elastic range, the following equation (Darendeli, 2001) fitting the laboratory data was used:

$$\frac{G}{G_0} = \frac{1}{1+(\frac{\gamma}{\gamma_r})^a} \qquad \text{(eq. 5)}$$

where a is the curvature parameter, γ_r is the reference strain.

The equation (5) is a revised version of the well-known hyperbolic relationship proposed by Hardin & Drnevich (1972):

$$\frac{G}{G_0} = \frac{1}{1+\frac{\gamma}{\gamma_r}} \qquad \text{(eq. 6)}$$

To include the effect of the stress level on the reference strain γ_r, Stokoe et al. (1999) proposed:

$$\gamma_r = \gamma_{r1}[\frac{p}{p_a}]^n \qquad \text{(eq. 7)}$$

which is used in this work in the following form:

$$\gamma_r = \gamma_{r1}[\frac{\sigma_v}{p_a}]^n \qquad \text{(eq. 8)}$$

where γ_{r1} is a reference strain when the vertical stress σ_v is 100kPa and n is the stress exponent.

RESULTS

Figures 3 and 4 present the measurements of the initial small-strain stiffness G_0 of soil, its degradation $G(\gamma)$ (Figure 3) and increase in the damping ratio $\mu(\gamma)$ (Figure 4) for vertical stress $б_v$ varying from 20 to 300kPa for all the conducted tests summarized in Table 4. When comparing the results from anisotropically and isotropically consolidated samples, one can see that the stiffness at the same vertical stresses is generally only slightly lower when the sample is under anisotropic consolidation (around 5% difference at higher vertical stresses, and up to 20% at lower vertical stresses). This happens even though the mean effective stresses can differ quite significantly. For example, for the vertical stress of σ_v=300kPa the mean effective stresses are p=188kPa and p=300kPa for anisotropically and isotropically consolidated samples, respectively, but the measured initial shear stiffnesses G_0 are only slightly lower in the case of the anisotropic consolidation. This means that the shear stiffness for vertically propagating waves depends primarily on the stress component in the direction of wave propagation (in this case σ_v) and less on the stress component perpendicular to the direction of the shear wave propagation (in this case σ_h). This is particularly visible when one compares the shear stiffness and its degradation for the anisotropically consolidated samples at σ_v=300kPa and p=188kPa (e.g., Tests 1.5 and 3.5) with isotropically consolidated samples at p=200kPa (e.g., Tests 2.4 and 4.4). Although the mean effective stress p is higher for the isotropically consolidated sample, the measured shear stiffness is noticeably lower (G_0 of around 100MPa versus nearly 120MPa for the anisotropically consolidated samples).

Figure 4 shows that the damping ratio $\eta(\gamma)$ reduces with the increasing mean effective stress p for all tested relative densities and consolidation types. Comparing the measurements from the same relative densities and either anisotropic or isotropic consolidation reveals that the damping ratio $\eta(\gamma)$ is reduced in isotropically consolidated samples (more distinct at lower σ_v, with slight difference at higher σ_v). Note that the threshold strain at which damping ratio $\eta(\gamma)$ starts to increase in Figure 4 is higher than the initiation in the shear stiffness degradation $G(\gamma)$ shown in Figure 3. Similar trends were found by others, e.g., Goudarzy et al. (2018a) suggesting that one can identify a nonlinear range of soil elastic behavior (where stiffness degrades but dissipation does not take place) which has been identified by others in the past research (e.g., Jardine, 1992).

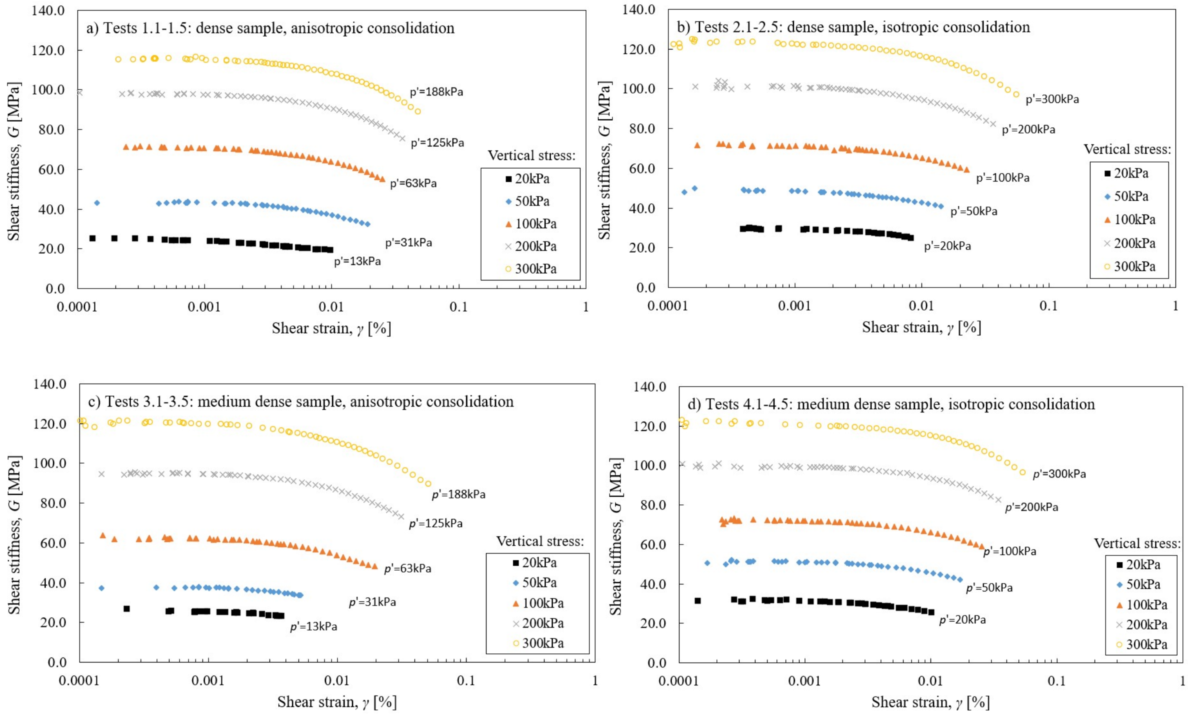

Fig. 3 Measurements of stiffness degradation *G(γ)* from resonant column tests: a) Tests 1.1-1.5: dense sand, anisotropic consolidation, b) Tests 2.1-2.5: dense sand, isotropic consolidation, c) Tests 3.1-3.5: medium dense sand, anisotropic consolidation, d) Tests 4.1-4.5: medium dense sand, isotropic consolidation.

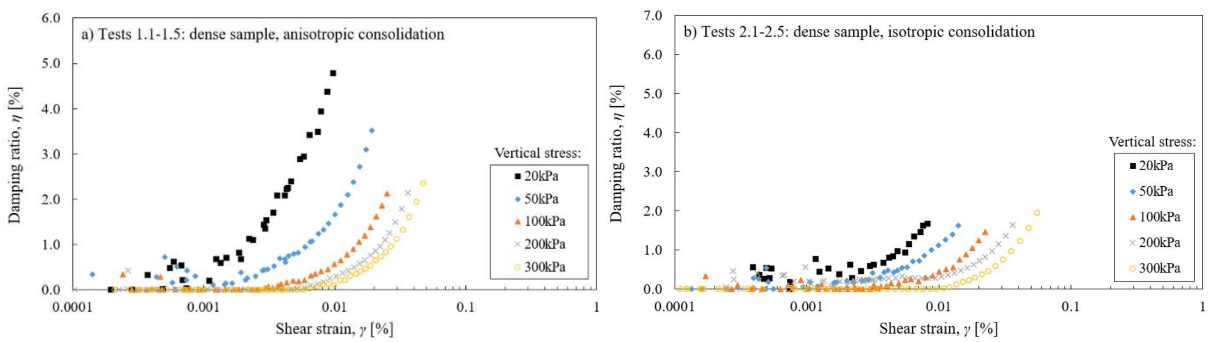

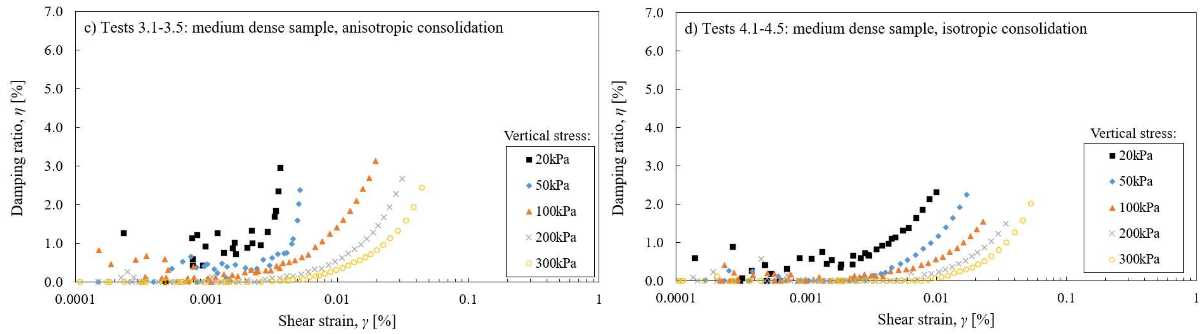

Fig. 4 Measurements of damping ratio *η(γ)* from resonant column tests: a) Tests 1.1-1.5: dense sand, anisotropic consolidation, b) Tests 2.1-2.5: dense sand, isotropic consolidation, c) Tests 3.1-3.5: medium dense sand, anisotropic consolidation, d) Tests 4.1-4.5: medium dense sand, isotropic consolidation.

Figure 5 presents relative shear stiffness degradation expressed as $G(\gamma)/G_0$. It can be observed how the rate of the shear stiffness degradation with the increasing strain level is affected by the stress level. The lower the vertical stress σ_v (and the mean effective stress p), the faster is the shear stiffness degradation as shown also in previous research works on sands (e.g., Tatsuoka et al., 1978; Seed et al., 1984; Oztoprak & Bolton, 2013). The recorded measurements are compared in Figure 5 with limiting envelopes from the past research: i) a lower bound limit from isotropically consolidated triaxial samples tested at the mean effective stress of 20kPa (Kokusho, 1980); and ii) an upper bound limit from resonant column tests on isotropically consolidated samples tested at the mean effective stress of 400kPa (Lanzano et al., 2016). This comparison shows that the obtained results generally fit between these lower and upper bounds.

Direct comparison of corresponding tests at the same vertical stress σ_v under anisotropic and isotropic consolidation is shown in Figure 6. The measurements for the tests at σ_v=20kPa (Figure 6a) lie closely to the lower bound given by Kokusho (1980) whereas the measurements for the tests at σ_v=300kPa (Figure 6e) lie closely to the upper bound given by Lanzano et al. (2016). Importantly, it is observed that the shear stiffness degradation $G(\gamma)/G_0$ is affected by the type of consolidation, with the tests under anisotropic consolidation generally having a faster rate of shear stiffness degradation with increasing shear strain than the corresponding samples under isotropic consolidation (the exception is the tests at a vertical stress of 20kPa, confirming the general observations that testing soils at low stress levels remains challenging). The relative density also affects the observed trends, with medium dense sand having on average a faster rate of the shear stiffness degradation (especially for the case of the tests under anisotropic consolidation).

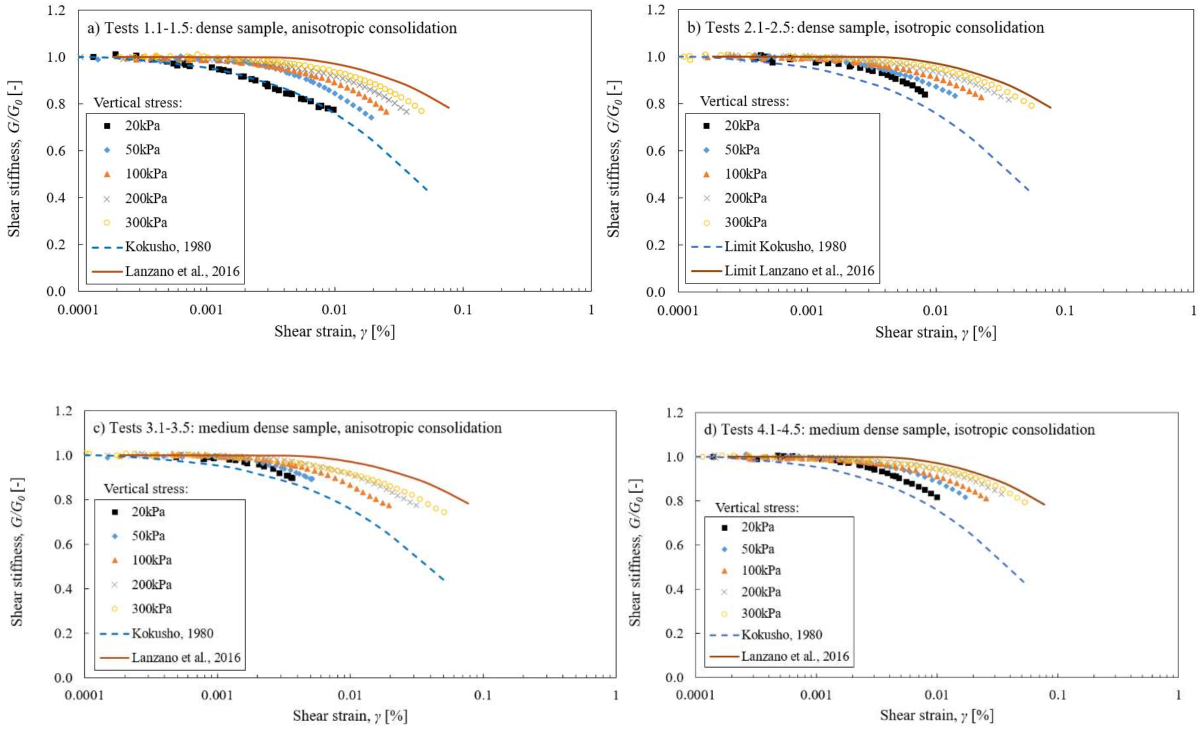

Fig. 5 Measurements of stiffness degradation $G(\gamma)/G_0$ from resonant column tests: a) Tests 1.1-1.5: dense sand, anisotropic consolidation, b) Tests 2.1-2.5: dense sand, isotropic consolidation, c) Tests 3.1-3.5: medium dense sand, anisotropic consolidation, d) Tests 4.1-4.5: medium dense sand, isotropic consolidation.

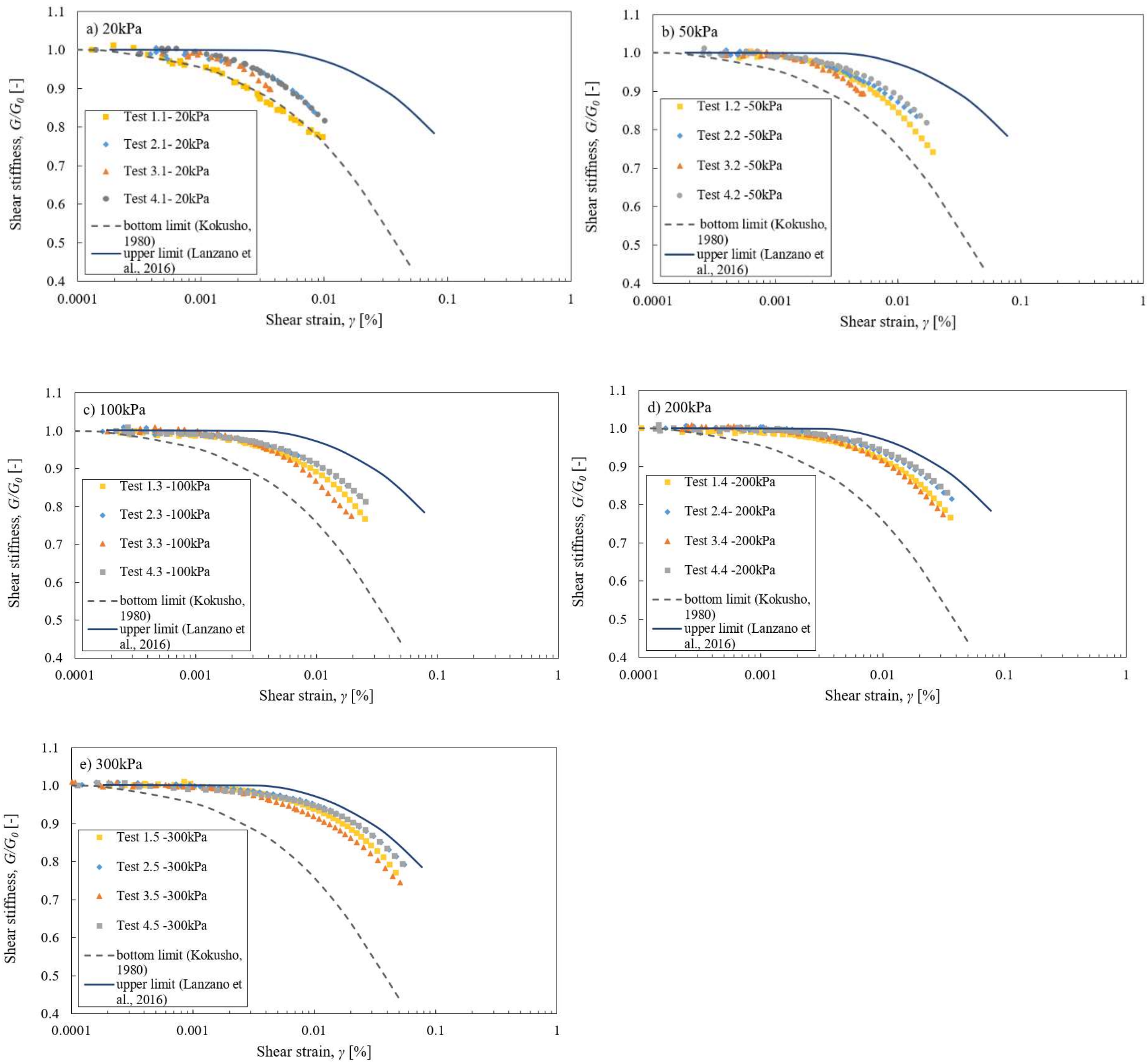

Fig. 6 Comparison of stiffness degradation $G(\gamma)/G_0$ from resonant column tests for: a) vertical stress σ_v of 20kPa, b) vertical stress σ_v of 50kPa, c) vertical stress σ_v of 100kPa, d) vertical stress σ_v of 200kPa, e) vertical stress σ_v of 300kPa.

The evaluation of the initial shear stiffness G_0 compared with selected analytical expressions is shown in Figure 7. The classical expression on the shear stiffness G_0 as a function of the mean effective stress p without considering the impact of stress components (equation 2) given by Hardin & Black (1966) has been calibrated against tests under isotropic consolidation (Figure 7b and d) and used subsequently to predict the G_0 shear stiffness under anisotropic consolidation (Figure 7a and c). This reveals that the classical approach underestimates the shear stiffness G_0 under anisotropic consolidation. In contrast, the expression by Yu & Richart (1984) shows matching the results of both, isotropically and anisotropically consolidated samples. The ratio of the fitting parameters for the vertical σ_v and horizontal σ_h stress components $\frac{n_1}{n_2}$ is from 2.5 (for dense samples) to 4.0 (for medium dense samples). This confirms that the vertical stress component is dominant in the G_0 shear stiffness characteristics in this study. In addition, the results of bender element tests, carried out in the past (Kassas et al., 2021), have been presented in Figure 7d for comparison, since conducted on isotropically consolidated samples of medium dense Hostun sand. Generally, only a slight discrepancy can be found between both, which confirms that the results obtained from resonant column tests can be considered reliable.

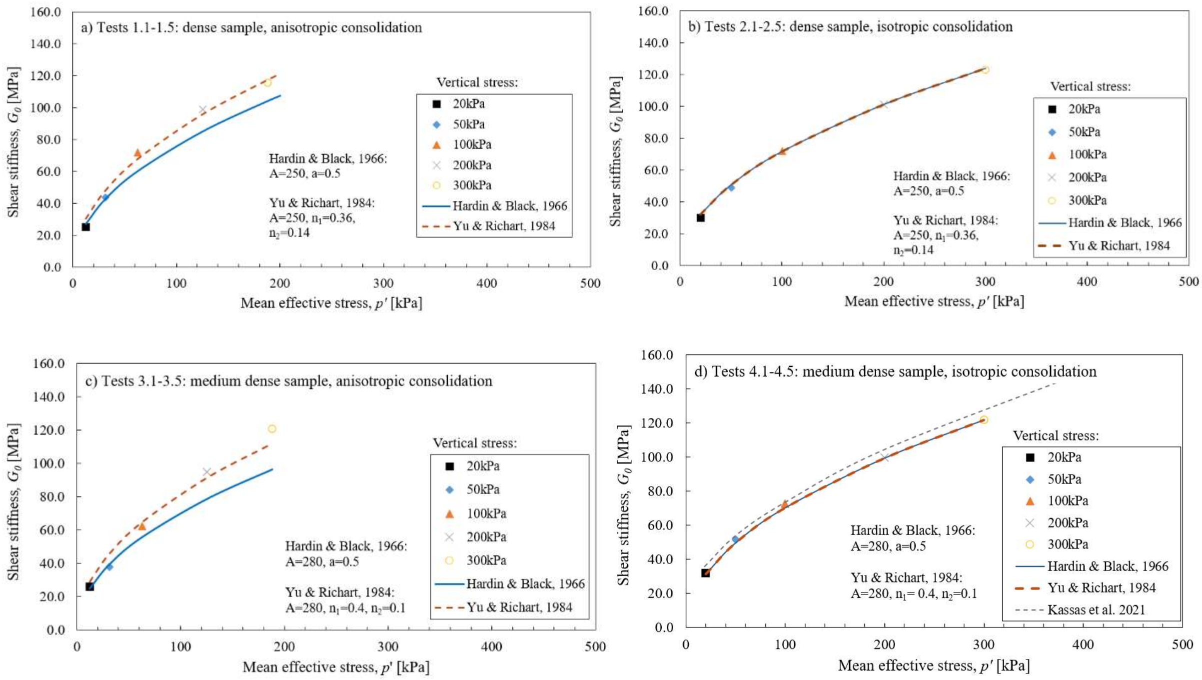

Fig. 7 Initial G_0 shear stiffness evaluated from resonant column tests: a) Tests 1.1-1.5 -dense sand, anisotropic consolidation, b) Tests 2.1-2.5 -dense sand, isotropic consolidation, c) Tests 3.1-3.5 -medium dense sand, anisotropic consolidation, d) Tests 4.1-4.5 -medium dense sand, isotropic consolidation.

Figure 8 presents the measured stress-strain curves in static torsional shear tests. These allow one-to-one comparisons for calibration of soil constitutive models in the future (although simplified calibration could be carried out from *G(γ)* curves, e.g., see Kowalczyk, 2020 where calibration was based on *G(γ)* curves proposed by Dietz & Muir Wood, 2007). One can observe in Figure 8 that the stiffness of isotropically consolidated samples at double strain amplitude up to 0.2% is slightly higher at each of the compared relative densities and vertical stresses, which is consistent with the results obtained from the resonant column tests (shown in Figures 5 and 6).

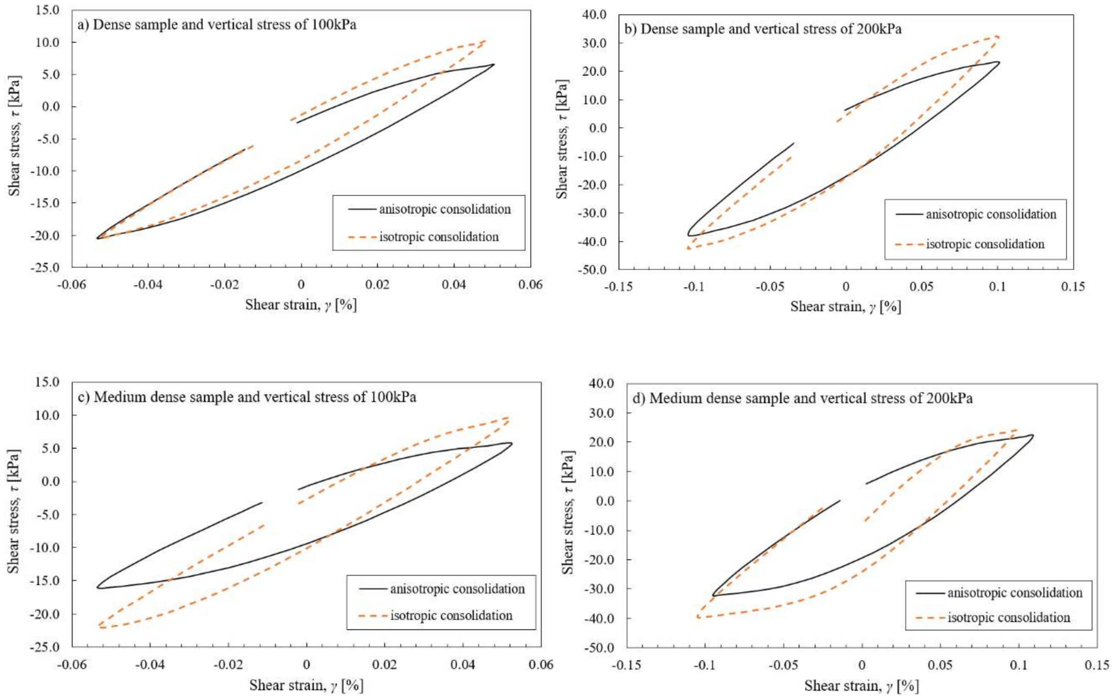

Fig. 8 Stress-strain behavior measured in torsional shear tests on samples under vertical stress σ_v of: a) 100kPa -dense sand, b) 200kPa -dense sand, c) 100kPa -medium dense sand, d) 200kPa -medium dense sand.

Figures 9 and 10 present the effect of overconsolidation imposed sometimes in centrifuge works when the same scaled model is spun at higher and, subsequently, lower N-g level (e.g., Lanzano et al., 2012). It can be observed that the effect of overconsolidation is not obvious at actual measurements of G_0 shear stiffness (i.e., no effect for dense sand -Fig. 9a; slight increase for medium dense sand -Fig. 10a). In contrast, the influence of overconsolidation can be noticed at larger strains, in which case the soil subjected to overconsolidation (and higher mean effective stress *p*) has a lower rate of shear stiffness degradation G/G_0 at corresponding shear strains (Fig. 9b and Fig. 10b). This is particularly visible in static torsional shear tests presented in Figures 9c and 10c, where the increase in shear stiffness in case of overconsolidated soil is clear.

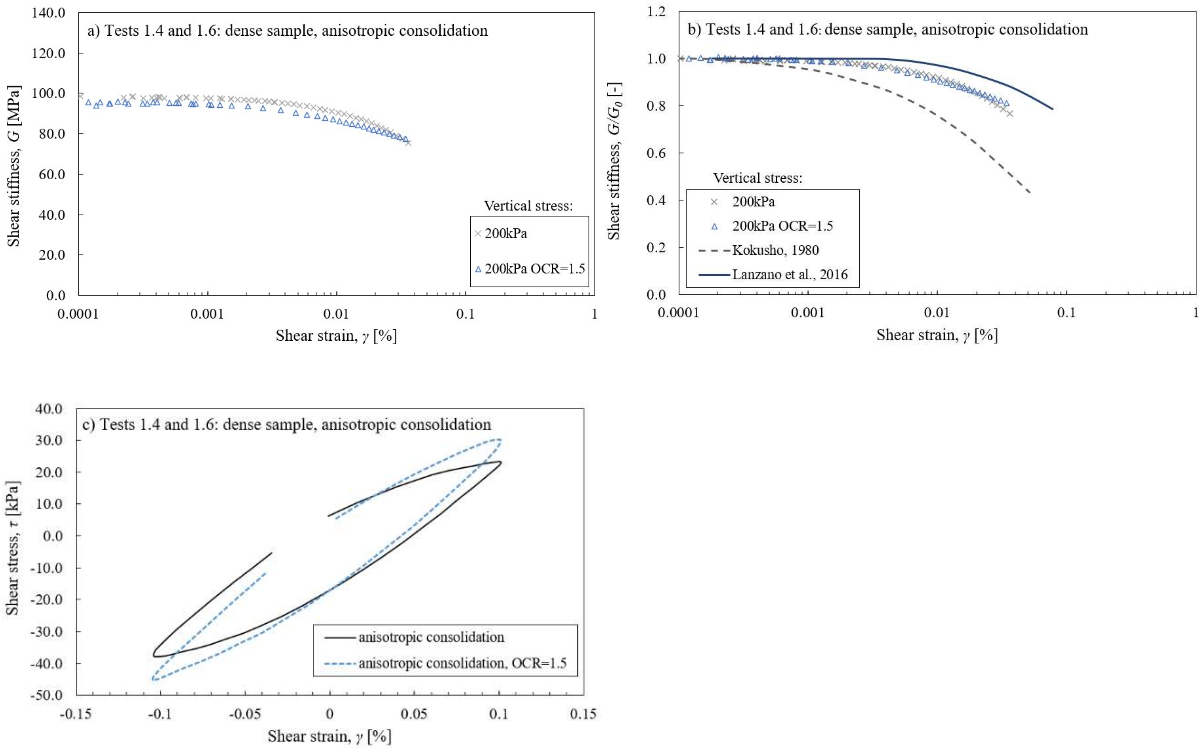

Fig. 9 Effect of overconsolidation of anisotropically consolidated dense sand: a) shear stiffness degradation $G(\gamma)$, b) normalized shear stiffness degradation $G(\gamma)/G_0$, c) stress-strain curves from torsional shear tests.

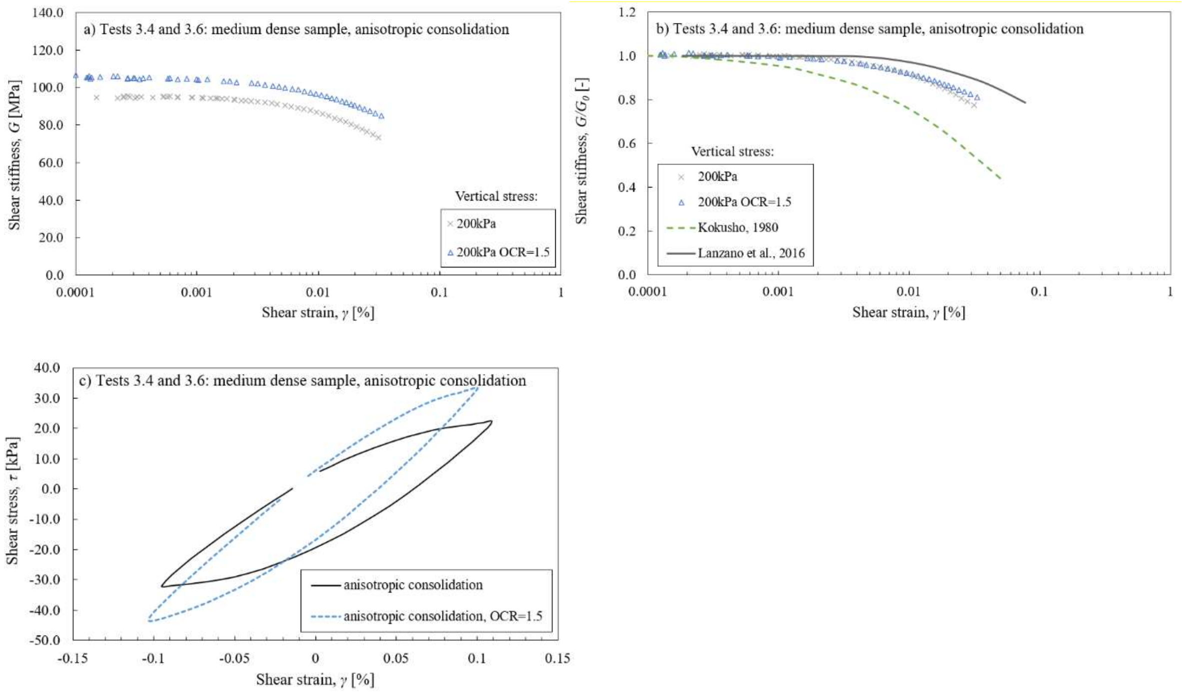

Fig. 10 Effect of overconsolidation of anisotropically consolidated medium dense sand: a) shear stiffness degradation *G(γ)*, b) normalized shear stiffness degradation *G(γ)/G₀*, c) stress-strain curves from torsional shear tests.

Figure 11 presents reference strain γ_r estimated from all the conducted tests. The reference strain γ_r in this work was estimated for the ratio of G/G_0=0.8 due to the study being focused on the small-strain range applicable to seismic loading. Fitting curves defined from equation 8 (Stokoe et al., 1999) have been also plotted in Figure 11. The reference strain for isotropically consolidated samples (dense and medium dense) are practically the same for the corresponding vertical stresses (thus only a single fitting curve is proposed for both). More scatter can be observed for anisotropically consolidated samples, where the medium dense sample has lower reference strains for the corresponding vertical stresses. In general, the reference strain is always lower for anisotropically consolidated soil than for isotropically consolidated soil, as already evident from Figures 5 and 6, showing a faster rate of stiffness degradation in anisotropically consolidated samples.

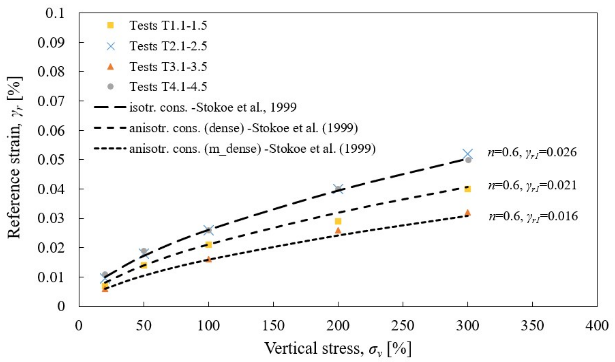

Fig. 11 Reference strain γ_r estimated from the laboratory data and compared with the analytical expressions by Stokoe et al. (1999).

Finally, Figure 12 shows shear stiffness degradation fitting curves evaluated from inserting equation 8 into equation 5, i.e.,:

$$\frac{G}{G_0} = \frac{1}{1+\left(\frac{\gamma}{\gamma_{r1}\left[\frac{\sigma_v'}{p_a}\right]^n}\right)^a} \qquad \text{(eq. 9)}$$

which can be used in simple constitutive models to model soil nonlinearity in seismic analysis and help calibrating advanced soil constitutive models for simulation of centrifuge tests or design predictive studies. Figure 12 shows that the calibration of eq. (9) differs for anisotropically and isotropically consolidated samples. Apart from γ_{r1} (seen to be different from plots in Figure 11), the exponent a also differs. The identified differences (i.e., the reference strain reduced to 80% and the exponent to 90% when compared with isotropically consolidated samples) can be treated as first approximation to determine shear stiffness G/G_0 degradation curves for other sands where data is available only for isotropic consolidation but one needs to have also data on anisotropic consolidation.

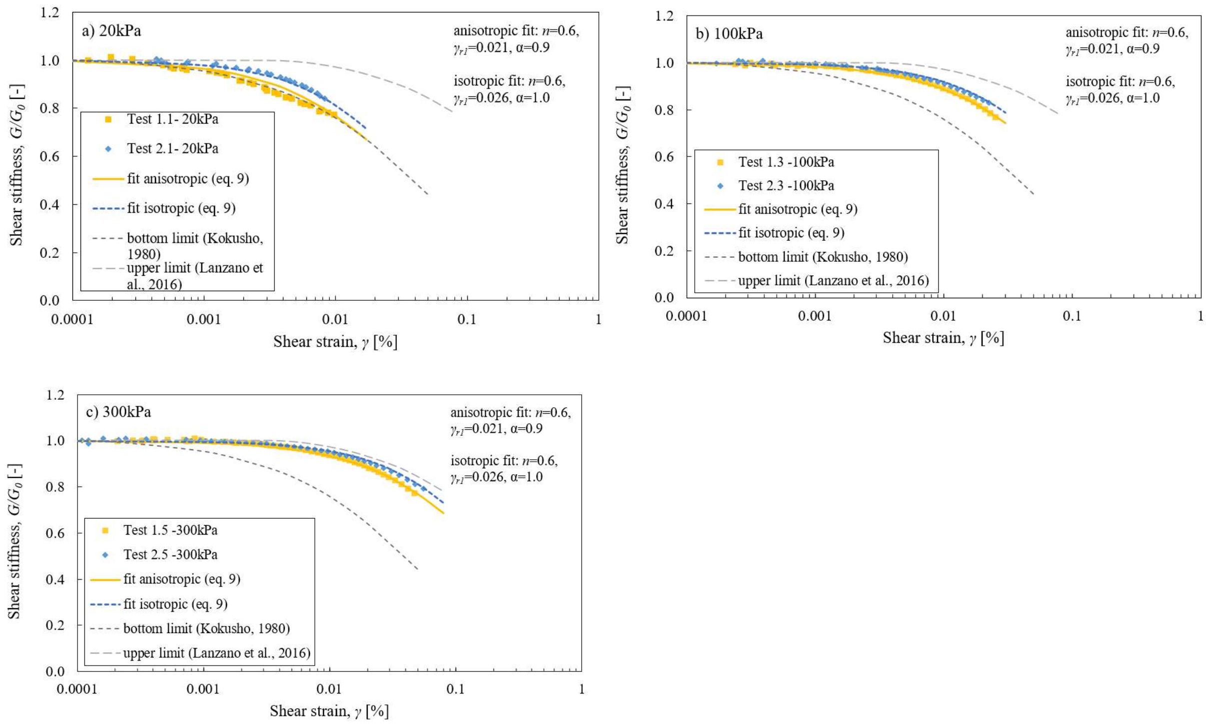

Fig. 12 Comparison of shear stiffness degradation G/G_0 from laboratory measurements and analytical expression (eq. 9): a) dense sand at vertical stress of 20kPa, b) dense sand at vertical stress of 100kPa, c) dense sand at vertical stress of 300kPa.

SUMMARY AND CONCLUSIONS:

This study presented a suite of torsional resonant column tests supported by static torsional simple shear tests aimed at characterization of the soil small-strain stiffness at truly anisotropic consolidation, thus highly relevant to support calibration of macroscopic continuum-based soil constitutive models in seismic applications. The measurements showed the differences in the small-strain shear stiffness obtained from anisotropically and isotropically consolidated samples of Hostun sand. The following are the most important findings:

- The initial shear stiffness G_0 is controlled primarily by the vertical stress component σ_v. As a result, when anisotropically and isotropically consolidated samples at the same vertical stress σ_v (but different mean effective stress p) are compared, the difference in the obtained G_0 stiffness, is typically relatively insignificant, ranging from 5% at higher stress levels to 20% at lower stress levels.

- The initial shear stiffness G_0 for both anisotropically and isotropically consolidated samples can be approximated by a simple analytical expression (Yu & Richart, 1984) differentiating contributions from the the vertical (n_1) and horizontal (n_2) stress components, with the ratio of the exponents n_1/n_2 being in the range of 2.5-4.0 for Hostun sand used in this study.
- The difference in the shear stiffness degradation G/G_0 between corresponding anisotropically and isotropically consolidated samples increases with increasing shear strain, with the reference shear strain γ_r being lower for the samples under anisotropic consolidation. The effect of faster stiffness degradation becomes more pronounced at larger strains, particularly when the corresponding stress-strain curves obtained from static torsional shear tests.
- The shear stiffness degradation G/G_0 can be represented by an analytical expression (in this work by equation 9, combining equations of Darendeli, 2001 and Stokoe et al., 1999), which can be used to facilite: i) calibration of soil constitutive models in the finite element modelling in earthquake geotechnical engineering and ii) first approximation of shear stiffness degradation of other sands than Hostun sand under anisotropic consolidation.
- Finally, for cases of soil overconsolidation, similar trends of relatively little influence on the initial shear stiffness G_0 but increasing importance with increasing shear strain on the shear stiffness degradation G/G_0 were found for anisotropically consolidated samples under an overconsolidation ratio of 1.5.

To sum up, this work has provided useful dataset for research works requiring calibration of soil constitutive models in finite element modelling on soil tests in the small strain range and subjected to truly anisotropic K_0 consolidation. In particular, the new dataset will be valuable when investigating shear wave propagation, such as in earthquake geotechnical engineering where numerical models are often developed to be complementary to centrifuge testing or when predictive numerical studies need to be developed at lower cost (i.e., without centrifuge testing). In addition, the presented results are also applicable to other boundary value problems within the small strains (e.g., in offshore or urban geotechnical engineering). The presented dataset will also be useful for validation and formulation of soil constitutive models on soil element tests when testing the ability of soil constitutive models to model simultaneously, i.e., with a single set of model parameters, soil mechanical behavior at isotropic and anisotropic consolidation pressures.

DATA AVAILABILITY STATEMENT:

Some or all data that support the findings of this study are available from the corresponding author upon reasonable request.

REFERENCES:

Abuhajar, O., El Naggar, H., Newson, T. (2015). Experimental and numerical investigations of the effect of buried box culverts on earthquake excitation. *Soil Dynamics and Earthquake Engineering* 79, 130-148. https://doi.org/10.1016/j.soildyn.2015.07.015

Adamidis, O., Alber, S. & Anastasopoulos, I. (2020). Assessment of 3D-2020 printing of granular media for geotechnical applications. *Geotechnical Testing Journal* 43(3), 641–659. DOI: 10.1520/GTJ20180259

Asia, Y. B., Madabhushi, G. S., Haigh, S. (2025). Deformation mechanisms of semi-integral bridge abutments in dry and saturated soil. *Géotechnique* 75(9), 1206–1217, doi: https://doi.org/10.1680/jgeot.24.01140

Benz, T. (2006). *Small-strain stiffness of soils and its numerical consequences*. PhD Thesis. University of Stuttgart, Germany.

Benz, T., Vermeer, P. A., Schwab, R. (2009). A small-strain overlay model. *International Journal of Numerical and Analytical Methods in Geomechanics* 33, 25–44. https://doi.org/10.1002/nag.701

Cilingir, U., Madabhushi, G. S. P. (2010). Effect of Depth on the Seismic Response of Circular Tunnels. *Canadian Geotechnical Journal* 48(1), 117-127. https://doi.org/10.1139/T10-047

Cilingir, U., Madabhushi, G. S. P. (2011). Effect of Depth on the Seismic Response of Square Tunnels. *Soils and Foundations* 51(3), 449-457. https://doi.org/10.3208/sandf.51.449

Dafalias, Y., F., Manzari, M. T. (2004). A simple plasticity sand model accounting for fabric change effects. *Journal of Engineering Mechanics* 130(6), 622-634. https://doi.org/10.1061/(ASCE)0733-9399(2004)130:6(622)

Darendeli, M. B. (2001). *Development of a New Family of Normalized Modulus Reduction and Material Damping Curves.* PhD Thesis. The University of Texas, Austin, Texas, US.

Deng, C., Haigh, S. K. (2021). Earth pressures mobilized in dry sand with active rigid retaining wall movement. *Géotechnique Letters* 11(3), 202-208. https://doi.org/10.1680/jgele.20.00116

Dietz, M., Muir Wood, D. (2007). Shaking table evaluation of dynamic soil properties. In the Proceedings of the 4th International Conference of Earthquake Geotechnical Engineering, 25-28 June, Thessaloniki, Greece.

Fioravante, V. (2000). Anisotropy of small strain stiffness of Ticino and Kenya sands from seismic wave propagation measured in triaxial tests. *Soils and Foundations* 40(4), 129-142. https://doi.org/10.3208/sandf.40.4_129

Fusco, A., Conti, R., Viggiani, G. M. B., Madabhushi, G. S. P., Prüm, C. (2024). Centrifuge and theoretical study of the seismic response of anchored steel sheet pile walls in dry sand. *Géotechnique* 74(13), 1561–1576. https://doi.org/10.1680/jgeot.22.00089

Goudarzy, M., König, D., Santamarina, J. C., Schanz, T. (2018a). The influence of the anisotropic stress state on the intermediate strain properties of granular material. *Géotechnique* 68(3), 221-232. https://doi.org/10.1680/jgeot.16.P.180

Goudarzy, M., König, D., Schanz, T. (2018b). Interpretation of small and intermediate strain characteristics of Hostun sand for various stress states. *Soils and Foundations* 58(6), 1526-1537. https://doi.org/10.1016/j.sandf.2018.09.002

Hardin, B.O., Black, W.L. (1966). Sand stiffness under various triaxial stresses. *Soils Mech. Found. Div.* 27–42. https://doi.org/10.1061/JSFEAQ.0000865

Hardin, B. O., Drnevich, V. P. (1972). Shear modulus and damping in soils. *J. Soil Mech. Found. Div. ASCE* 98, No. 7, 667–692. https://doi.org/10.1061/JSFEAQ.0001756

Hashash, Y. M., Philips, C., Groholski, D. R. (2010). Recent advances in non-linear site response analysis. In the Proceedings of 5th International Conference on Recent Advances in Geotechnical Earthquake Engineering and Soil Dynamics, San Diego, California (US).

He, B., Zhang, J.-M., Li, W., Wang, R. (2020). Numerical analysis of LEAP centrifuge tests on sloping liquefiable ground: Influence of dilatancy and post-liquefaction shear deformation. *Soil Dynamics and Earthquake Engineering* 137, 106288. https://doi.org/10.1016/j.soildyn.2020.106288

Jaky, J. (1948). Pressure in silos. In the Proceedings of 2nd International Conference on Soil Mechanics and Foundation Engineering, Rotterdam, Netherlands, vol. 1: 103-107.

Jardine, R. (1992). Some observations on the kinematic nature of soil stiffness. *Soils and Foundations* 32(2), 111-124. https://doi.org/10.3208/sandf1972.32.2_111

Kassas, K., Adamidis, O., Gerolymos, N., Anastasopoulos, I. (2021). Numerical modelling of a structure with shallow strip foundation during earthquake-induced liquefaction. *Géotechnique* 71(12), 1099-1113. https://doi.org/10.1680/jgeot.19.P.277

Kokusho, T. (1980). Cyclic triaxial test of dynamic soil properties for wide strain range. *Soils and Foundations* 20(2), 45-60. https://doi.org/10.3208/sandf1972.20.2_45

Kowalczyk, P. (2020). *Validation and application of advanced soil constitutive models in numerical modelling of soil and soil-structure interaction under seismic loading*. PhD Thesis, University of Trento, Italy. DOI: http://hdl.handle.net/11572/275675

Kowalczyk, P., Gajo, A. (2023). Introductory consideration supporting the idea of the release of elastic waves in hysteretic soil. *Open Geomechanics* 4(4), 1-25. https://doi.org/10.5802/ogeo.16

Kowalczyk, P., Madhusudhan, B. (2025). Mechanical behaviour of sand in simple shear at low stress levels and small strains. *Géotechnique Letters* 15(4), 266-276. https://doi.org/10.1680/jgele.24.00149

Lanzano, G., Bilotta, E., Russo, G., Silvestri, F., Madabhushi, S. P. G. (2012). Centrifuge modelling of seismic loading on tunnels in sand. *Geotechnical Testing Journal* 35(6), 854–869. DOI: 10.1520/GTJ104348

Lanzano, G., Visone, C., Bilotta, E., Santucci de Magistris, F. (2016). Experimental assessment of the stress-strain behaviour of Leighton Buzzard sand for the calibration of a constitutive model. *Geotechnical and Geological Engineering* 34(4), 991-1012. https://doi.org/10.1007/s10706-016-0019-5

Lbibb, S., Manzari, M. T. (2023). Stress-strain behavior of Ottawa sand in cyclic direct simple shear and modeling of cyclic strength using Artificial Neural Networks. *Soil Dynamics and Earthquake Engineering* 164, 107585. https://doi.org/10.1016/j.soildyn.2022.107585.

Madabhushi, S.S.C., Haigh, S. K. (2019). Centrifuge testing of dual row retaining walls in dry sand: The influence of earthquake sequence and multiple flights. *Soil Dynamics and Earthquake Engineering* 125, 105690. https://doi.org/10.1016/j.soildyn.2019.05.029.

Madabhushi, S.S.C., Haigh, S. K. (2022). On the dynamic response of flexible dual-row retaining walls in dry sand. *Géotechnique* 72(11), 941-956. https://doi.org/10.1680/jgeot.19.P.189

Madabhushi, S.S.C., Westcott, J. (2024). An Alternative Approach to Dynamic Earth Pressure Coefficients to Improve the Seismic Limit State Design of Earth-Retaining Structures. *Journal of Geotechnical and Geoenvironmental Engineering* 150(10), 1-17. https://doi.org/10.1061/JGGEFK.GTENG-12243

Mercado, V., Duque, J., El-Sekelly, W. (2024). Numerical modelling of LEAP-2022 dynamic centrifuge tests adopting a multi-surface plasticity model. *Soil Dynamics and Earthquake Engineering* 181, 108674. https://doi.org/10.1016/j.soildyn.2024.108674.

Morley, D. G., Madabhushi, G. S. P., Sakufiwa, D., Thusyanthan, I. (2024). Investigation into soil ratcheting behind integral bridges using centrifuge modelling. *Proceedings of the Institution of Civil Engineers - Bridge Engineering* 178(4), 373-389. https://doi.org/10.1680/jbren.23.00046

Oztoprak, S., Bolton, M. D. (2013). Stiffness of sands through a laboratory test data base. *Géotechnique* 63(1), 54-70. https://doi.org/10.1680/geot.10.P.078

Özcebe, A.G., Giretti, D., Bozzoni, F., Fioravante, V., Lai, C. G. (2021). Centrifuge and numerical modelling of earthquake-induced soil liquefaction under free-field conditions and by considering soil–structure interaction. *Bulletin of Earthquake Engineering* 19, 47–75. https://doi.org/10.1007/s10518-020-00972-3

Payan, M., Senetakis, K., Khoshghalb, A., Khalili, N. (2016). Influence of particle shape on small-strain damping ratio of dry sands. *Géotechnique* 66(7), 610–616. https:// doi.org/10.1680/jgeot.15.T.035.

Rohilla, S., Sebastian, R. (2023). Resonant column and cyclic torsional shear tests on Sutlej River sand subjected to the seismicity of Himalayan and Shivalik hill ranges: A case study. *Soil Dynamics and Earthquake Engineering* 166, 107766. https://doi.org/10.1016/j.soildyn.2023.107766

Santamarina, J. C., Cascante, G. (1996). Stress anisotropy and wave propagation: a micromechanical view. *Canadian Geotechnical Journal* 33, 770-782. https://doi.org/10.1139/t96-102-323

Seed, H. B., Wong, R., Idriss, I., Tokimatsu, K. (1984). Moduli and damping factors for dynamic analyses of cohesionless soils. Report No. UCB/EERC-84/14. Berkley, CA, USA: University of California.

Stokoe, K., Darendeli, M., Andrus, R. & Brown, L. (1999). Dynamic soil properties: laboratory, field and correlation studies. Proc. 2nd Int. Conf. Earthquake Geotech. Engg, 811-846.

Tatsuoka, F., Iwasaki, T., Takagi, Y. (1978). Hysteretic damping of sands under cyclic loading and its relation to shear modulus. *Soils and Foundations* 18(2), 25-40.

Tsinidis, G., Pitilakis, K., Madabhushi, G., Heron, C. (2015). Dynamic response of flexible square tunnels: centrifuge testing and validation of existing design methodologies. *Géotechnique* 65(5), 401–417. http://dx.doi.org/10.1680/geot.SIP.15.P.004

Wei, S., Liang, F., Wang, C., Yan, S. (2026). Centrifuge experimental study on the seismic response of a shallow-buried underground structure under varying ground motion characteristics. *Soil Dynamics and Earthquake Engineering* 203, 110092. https://doi.org/10.1016/j.soildyn.2026.110092.

Werden, S. K., Drnevich, V. P., Hall, J. R., Hankour, C., Conlee, C. T., Marr, A. W. (2013). New Approach to Resonant Column Testing. *Geotechnical Testing Journal* 36(2), 169-177. doi:10.1520/GTJ20120122

Wichtmann, T., Triantafyllidis, Th. (2016). An experimental data base for the development, calibration and verification of constitutive models for sand with focus to cyclic loading. Part II: tests with strain cycles and combined loading. *Acta Geotechnica* 11(4), 763-774. DOI:10.1007/s11440-015-0412-x

Wichtmann, T., Fuentes, W. and Triantafyllidis, T. (2019). Inspection of Three Sophisticated Constitutive Models Based on Monotonic and Cyclic Tests on Fine Sand: Hypoplasticity vs. Sanisand vs. ISA. *Soil Dynamics and Earthquake Engineering* 124, 172–183. doi:10.1016/j.soildyn.2019.05.001.

Yu, P., Richart, F. (1984). Stress ratio effects on shear modulus of dry sands. *Journal of Geotechnical Engineering* 110, 331–345. https://doi.org/10.1061/(ASCE)0733-9410(1984)110:3(331)